Evolution and exact eigenstates of a resonant quantum system

Shau-Jin Chang and Kang-Jie Shi
Department of Physics, University of Illinois at Urbana-Champaign, 1110 West Green Street, Urbana, Illinois 61801
(Received 20 November 1985)

We consider the generalized quantum Chirikov map under a resonance condition $2\pi\hbar = M/N$. This is the quantum-resonance condition discovered by Casati *et al.* At the resonance, the quantum system reduces to a set of independent $N \times N$ unitary matrix eigenequations. We can reduce the evolution operator of the original system as a direct sum of these $N \times N$ unitary matrices. We then obtain the eigenstates and eigenenergies (the pseudoenergies) of the quantum map and illustrate their dependences on a number of parameters. We plot these eigenstates in the coherent-state representation and show that they follow closely the Kolmogorov-Arnol'd-Moser curves and other classical orbits.

I. INTRODUCTION

One of the most studied area-preserving iterative systems is the Chirikov (standard) map.[1] We may obtain this map from a periodically kicked free rotor with the amplitude of the kick being a periodic function of the rotation angle. When the kick amplitude is zero, the system is integrable. For small but finite kicks, the system is a mixture of quasiperiodic solutions and chaotic regions. These quasiperiodic solutions are the well-known Kolmogorov-Arnol'd-Moser (KAM) trajectories.[2] For strong kicks and based on numerical studies, the system appears to be ergodic. This standard map has served as a testing ground for many theoretical ideas.

The introduction of quantum mechanics into a Chirikov map leads to many additional features. The quantum Chirikov map describes the qualitative behavior of atoms and molecules under the radiation of a laser beam. It may also predict the quantum stability of particle beams in an accelerator.[3]

Casati, Chirikov, Izraelev, and Ford made an important discovery of quantum resonance in the quantum Chirikov map.[4–6] When the external frequency and natural quantum frequency have simple rational ratios, they discovered numerically that the average energy of the system increases quadratically in time. This quadratic increment in energy is true for all coupling strength k, while the energy of the classical system is bounded for small k. Based on an analogy to Anderson localization, Grempel *et al.* suggested that the irrational cases should lead to states localized in p space and hence must have bounded energies.[7,8]

Recently, Casati and Guarneri made an important discovery of the existence of nonresonant and nonrecurrent behavior of kicked quantum rotors.[9] Up to the time of their discovery, it was a general belief that there are no possibilities for a periodically driven quantum system to be anything other than resonance and recurrence.[10] Casati and Guarneri showed rigorously that there is a third possibility: For a generic choice of the potential $V(q)$ there is a nonempty set of nonresonant values of the external frequency, sufficiently close to the rationals, such that the quasienergy spectrum still has a continuous component.

There are many other studies about how a quantum system should behave. Using semiclassical method, Barry *et al.* concluded that the Wigner function[11] of a quantum eigenstate must lie on a classical invariant manifold.[12] As we shall see, a coarse graining of the Wigner functions is necessary to achieve the quantum-to-classical transition.

The evolution operator under the quantum-resonance condition can be reduced into a set of finite matrix eigenequations. We then diagonalize these matrix equations, and obtain the eigenvalues (pseudoenergies) and eigenfunctions of the original problem. In a separate paper, we shall work out the propagation of a localized state, and study a nonresonance condition as a sequence of resonance conditions.[13] A brief summary of our results is presented in Ref. 14.

This paper is organized as follows. In Sec. II, we study the evolution operator and its matrix elements for a generalized quantum Chirikov map. In Sec. III, we impose the resonance condition, and reduce the evolution operator into a set of $N \times N$ unitary matrices. These two sections contain a short survey of essentially the same mathematical treatment as given by Izrailev and Shepelyanskii in Ref. 5. We include some detailed formulas which are necessary for our applications. In Sec. IV, we introduce the coherent-state representation and show that they are the coarse-grained Wigner functions. In Sec. V, we obtain the pseudoenergies and eigenfunctions by diagonalizing these $N \times N$ matrices numerically. We describe the pseudoenergies and eigenfunctions for reducible fractions in an Appendix.

II. EVOLUTION OPERATOR

The model that we shall study is the quantum Chirikov map and its generalization.[1] We consider both the classical and the quantum map generated by a periodically kicked free rotor with the Hamiltonian

$$H = \frac{p^2}{2} + V(q) \sum_n \delta(t-n) , \tag{2.1}$$

where the potential is periodic in q,

$$V(q+1) = V(q) . \tag{2.2}$$

We denote the coordinate at the kick $t=n$ as q_n, and the momentum just before and after the kick as p_n and p_{n+1}, respectively. (See Fig. 1.) The p_n and q_n obey the discrete equations

$$p_{n+1}=p_n-V'(q_n)\ , \tag{2.3}$$

$$q_{n+1}=q_n+p_{n+1}(\mathrm{mod}\ 1)\ . \tag{2.4}$$

If we choose $V(q)$ to be $k\,[\cos(2\pi q)]/(2\pi)^2$, then, Eq. (2.3) reduces to

$$p_{n+1}=p_n+\frac{k}{2\pi}\sin(2\pi q_n)\ . \tag{2.5}$$

Equations (2.5) and (2.4) are the familiar Chirikov equations.

To describe a quantum system, we need to impose the quantization rule. The quantization rule for the discrete system (2.3),(2.4) is[15]

$$[p_n,q_n]=-i\hbar\ . \tag{2.6}$$

To relate (p,q) from time t to $t+1$, we introduce a unitary evolution operator

$$U=e^{-(i/2\hbar)p_n^2}e^{-(i/\hbar)V(q_n)}\ . \tag{2.7}$$

It is straightforward to show that

$$p_{n+1}=U^{-1}p_nU,\quad q_{n+1}=U^{-1}q_nU\ . \tag{2.8}$$

Indeed, Eqs. (2.7) and (2.8) and the quantization relation (2.6) imply the equations of motion (2.3) and (2.4).

We introduce the eigenstate of the evolution operator by

$$U\,|\,\psi\rangle=e^{-i\omega}\,|\,\psi\rangle\ . \tag{2.9}$$

Since U is unitary, its eigenvalues are pure phases as indicated in (2.9). The factor $e^{-i\omega}$ is the analog of $e^{-iEt/\hbar}$. The quantity ω (or more precisely $\hbar\omega$) is known as the pseudoenergy, and is only determined up to mod(2π).

Since q is periodic, the eigenvalues for the momentum p are discrete. We denote the momentum eigenstates by $\langle m\,|$ which obeys

$$\langle m\,|p=2\pi\hbar m\langle m\,|\ . \tag{2.10}$$

Multiplying Eq. (2.9) by $\langle m\,|$, we have

$$\sum_{m'=-\infty}^{\infty}U_{mm'}\phi_{m'}=e^{-i\omega}\phi_m\ , \tag{2.11}$$

where ϕ_m is the wave function in p space, and $U_{mm'}$ is the matrix element of U in p space.

For the Chirikov map, Izrailev and Shepelyanskii have worked out $U_{mm'}$ explicitly as

$$U_{mm'}=e^{-i2\pi^2m^2\hbar}(-i)^{m'-m}J_{m'-m}(z)\ , \tag{2.12}$$

with

$$z=\frac{k}{(2\pi)^2\hbar}\ . \tag{2.13}$$

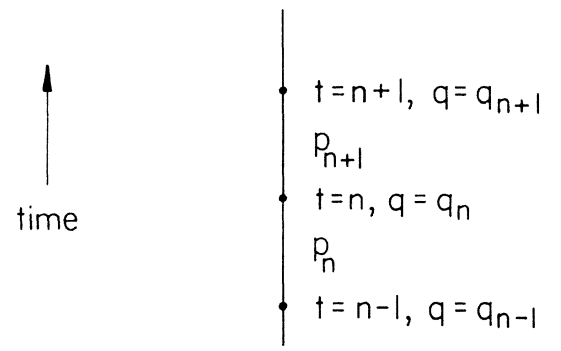

FIG. 1. The coordinate at the kick at $t=n$ is q_n, and the momenta just before and after the kick are p_n and p_{n+1}, respectively.

III. REDUCTION OF $U_{mm'}$

A. Resonance condition

As a classical iterative system,

$$p_{n+1}=p_n-V'(q_n)\ ,$$

$$q_{n+1}=q_n+p_{n+1}(\mathrm{mod}\ 1)$$

are invariant under the transformation

$$p\rightarrow p+M\ , \tag{3.1}$$

where M is an integer. If such a symmetry also exists in the quantum system,[16] it corresponds to a transformation in the momentum eigenvalue m by

$$m\rightarrow m+\frac{M}{2\pi\hbar}\ . \tag{3.2}$$

Since the eigenvalue m is an integer, Eq. (3.2) can be valid only if

$$\frac{M}{2\pi\hbar}=N \tag{3.3}$$

is an integer, or equivalently, only if

$$2\pi\hbar=M/N \tag{3.4}$$

is a rational number. The condition that $2\pi\hbar$ is a rational number is the resonance condition discussed in Ref. 4. In our convention, $2\pi\hbar$ is the ratio of the natural quantum frequency $\omega=4\pi^2\hbar$ and the driving frequency $\Omega=2\pi$.[17]

Under (3.4), the symmetry condition (3.2) becomes

$$m\rightarrow m+N\ . \tag{3.5}$$

It is straightforward to show that the matrix element for the displaced m's obeys

$$U_{m+N,m'+N}=e^{-i\pi M(2m+N)}U_{mm'}$$

$$=(-1)^{MN}U_{mm'}\ . \tag{3.6}$$

There are two possibilities: (1) At least one of M and N is even. (2) Both M and N are odd. We consider the first case here. We shall leave the second case in the Appendix.

B. Reduction to $N\times N$ matrices

In case (1) mentioned above, we have $MN=$even, and

$$U_{m+N,m'+N}=U_{mm'} . \tag{3.7}$$

Introducing

$$m=s+Nl,\quad 1\le s\le N,\quad -\infty<l<\infty \tag{3.8}$$

we have the general form of an eigenfunction as

$$\phi_{s+Nl}=e^{-ial}[\phi(a)]_s,\quad 0\le a<2\pi \tag{3.9}$$

where ϕ_m obeys

$$\phi_{m+N}=e^{-ia}\phi_m . \tag{3.10}$$

The variable a $(0\le a<2\pi)$ is the analog of the wave vector k in Bloch wave. In terms of the $N\times N$ matrix

$$[U(a)]_{ss'}\equiv\sum_{l'}U_{s,s'+Nl'}e^{-ial'} , \tag{3.11}$$

we can show that

$$\sum_{s'}[U(a)]_{ss'}\phi(a)_{s'}=e^{-i\omega(a)}[\phi(a)]_s . \tag{3.12}$$

In other words, $\phi(a)$ is the eigenvector of the $N\times N$ matrix $U(a)$ with the same eigenvalue $e^{-i\omega(a)}$. It is straightforward to show that $U(a)$ is unitary in the $N\times N$ space.

Thus, the original problem of finding the eigenvalues and eigenstates of an $\infty\times\infty$ matrix U is reduced to that of finding the eigenvalues and eigenstates of $N\times N$ matrices $U(a)$.[5]

We can express the transformation property of an arbitrary wave function under U in terms of the transformation properties of $N\times N$ matrices as

$$(U\psi)_{s+Nl}=\int_0^{2\pi}\frac{da}{2\pi}e^{-ial}[U(a)\psi(a)]_s , \tag{3.13}$$

$$(U^n\psi)_{s+Nl}=\int_0^{2\pi}\frac{da}{2\pi}e^{-ial}[U^n(a)\psi(a)]_s , \tag{3.14}$$

where

$$[\psi(a)]_s\equiv\sum_l\psi_{s+Nl}e^{ial} , \tag{3.15}$$

and

$$\psi_{s+Nl}=\int_0^{2\pi}\frac{da}{2\pi}e^{-ial}[\psi(a)]_s . \tag{3.16}$$

Thus we can obtain the iterative property of ψ_m, $-\infty<m<\infty$, from the iterative property of $\psi(a)_s$, $1\le s\le N$. Note that we can invert (3.11) to give

$$U_{s+Nl,s'+Nl'}=\int_0^{2\pi}\frac{da}{2\pi}e^{-ia(l-l')}[U(a)]_{ss'} . \tag{3.17}$$

C. Explicit evaluation of $U(a)$

From Eqs. (2.7), we obtain

$$U_{mm'}=e^{-i2\pi^2m^2\hbar}\int_0^1 dq\, e^{-(i/\hbar)V(q)}e^{-i2\pi(m-m')q} . \tag{3.18}$$

Under the condition

$$2\pi\hbar=M/N \text{ and } MN=\text{even} , \tag{3.19}$$

we obtain

$$U_{s+Nl,s'+Nl'}=e^{-i2\pi^2s^2\hbar}\int_0^1 dq\, e^{-(i/\hbar)V(q)}e^{-i2\pi(s-s')q}\times e^{-i2\pi(l-l')Nq} . \tag{3.20}$$

Now, we are ready to compute $U(a)$,

$$U(a)_{ss'}=\sum_{l'}U_{s,s'+Nl'}e^{-ial'}=e^{-i2\pi^2s^2\hbar}\int_0^1 dq\, e^{-(i/\hbar)V(q)}e^{-i2\pi(s-s')q}\sum_{l=-\infty}^{\infty}e^{-ial+i2\pi lNq} . \tag{3.21}$$

To simplify (3.21), we make use of the Poisson summation formula[18]

$$\sum_{l=-\infty}^{\infty}e^{2\pi il\phi}=\sum_{j=-\infty}^{\infty}\delta(\phi-j) , \tag{3.22}$$

and obtain

$$[U(a)]_{ss'}=e^{-i2\pi^2s^2\hbar}e^{i(s'-s)a/N}\times\frac{1}{N}\sum_{j=1}^{N}\exp\left[-\frac{i}{\hbar}V\left(\frac{a}{2\pi N}+\frac{j}{N}\right)+\frac{i2\pi(s'-s)j}{N}\right] . \tag{3.23}$$

In particular, for a Chirikov map, we have

$$U(a)_{ss'}=\frac{1}{N}\exp[-i2\pi^2s^2\hbar+i(s'-s)a/N]\times\sum_{j=1}^{N}\exp\left[\frac{i2\pi(s'-s)j}{N}-iz\cos\left[\frac{2\pi j+a}{N}\right]\right] , \tag{3.24}$$

where

$$z\equiv\frac{k}{(2\pi)^2\hbar} . \tag{3.25}$$

The finite $N\times N$ matrix $U(a)$ involves only elementary functions. From (3.23), we note that $U(a)$ depends only on $V(q)$ at

$$2\pi q=\frac{a}{N}+\frac{2\pi j}{N},\quad j=1,2,\ldots,N . \tag{3.26}$$

Since $2\pi q$ describe angles, we can represent them as points on a unit circle. They form N equally-spaced points with the initial point $2\pi q_0$ $(=2\pi q_n)$ located at a/N, as shown in Fig. 2. Under the operation of U and for a fixed a, only N discrete values of q are involved and map into each other. The q's associated with different a's never mix.

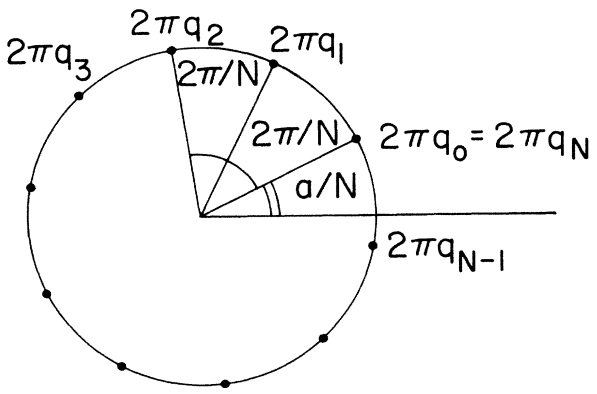

FIG. 2. The $N\times N$ unitary matrix $U(a)$ depends only on $V(q)$ at N equally-spaced points with the initial point $q_0\equiv a/2\pi N$, and spacing $1/N$. They are represented here as N points on a unit circle.

$$\langle q\,|\,\alpha\rangle=\left[\frac{\omega}{\pi\hbar}\right]^{1/4}e^{-|\alpha|^2/2+\alpha^2/2}\exp[-(\sqrt{\omega/2\hbar}q-\alpha)^2]$$
$$=\left[\frac{\omega}{\pi\hbar}\right]^{1/4}e^{-i\alpha_1\alpha_2}\exp[-(\sqrt{\omega/2\hbar}q-\alpha_1)^2+2i\alpha_2\sqrt{\omega/2\hbar}q]\,, \quad (4.5a)$$

$$\langle p\,|\,\alpha\rangle=\left[\frac{1}{\pi\hbar\omega}\right]^{1/4}e^{-|\alpha|^2/2-\alpha^2/2}\times\exp\left[-\left[\frac{p}{\sqrt{2\hbar\omega}}+i\alpha\right]^2\right]$$
$$=\left[\frac{1}{\pi\hbar\omega}\right]^{1/4}e^{i\alpha_1\alpha_2}\exp\left[-\left[\frac{p}{\sqrt{2\hbar\omega}}-\alpha_2\right]^2-\frac{2i\alpha_1 p}{\sqrt{2\hbar\omega}}\right]. \quad (4.5b)$$

IV. COHERENT-STATE REPRESENTATION AND COARSE-GRAINED WIGNER FUNCTIONS

A. Coherent-state representation

To compare the quantum states with the classical states, we describe the quantum states in the coherent-state representation.[19] In the following, we review briefly several important results of the coherent-state representation.

A coherent state $|\alpha\rangle$ is an eigenstate of the annihilation operator a,

$$a\,|\alpha\rangle=\alpha\,|a\rangle\,, \quad (4.1)$$

where the annihilation and the creation operators are

$$a\equiv\frac{\omega q+ip}{\sqrt{2\hbar\omega}}\,, \quad (4.2a)$$

$$a^\dagger\equiv\frac{\omega q-ip}{\sqrt{2\hbar\omega}}\,. \quad (4.2b)$$

In this section, ω denotes a conveniently chosen natural frequency. Please do not confuse it with pseudoenergy. The annihilation and the creation operators obey the quantization rule

$$[a,a^\dagger]=1\,. \quad (4.3)$$

The eigenvalue α is complex,

$$\alpha=\alpha_1+i\alpha_2\,. \quad (4.4)$$

In (4.2), we assume that p and q have the range $-\infty$ to ∞.

By comparing (4.2) and (4.4), we may identify naively the real part α_1 as $q\sqrt{\omega/2\hbar}$ and the imaginary part α_2 as $p/\sqrt{2\hbar\omega}$. Since p and q do *not* commute, these identifications are necessarily imprecise.

To understand the coherent state precisely, we compute its q- and p-space wave functions $\langle q\,|\,\alpha\rangle$ and $\langle p\,|\,\alpha\rangle$, obtaining

Equations (4.5) indicate that the coherent state gives a Gaussian distribution in both q and p space, is centered at $(\sqrt{2\hbar/\omega}\alpha_1,\sqrt{2\hbar\omega}\alpha_2)$, and has widths $\sqrt{\hbar/2\omega}$ and $\sqrt{\hbar\omega/2}$, respectively. This wave packet has a minimal combined width $\Delta p\Delta q=\hbar/2$.

The coherent states are overcomplete. Two coherent states $|\alpha\rangle$ and $|\beta\rangle$ with eigenvalues α and β are not orthogonal, but obey

$$\langle\alpha\,|\,\beta\rangle=\exp(\alpha^*\beta-\tfrac{1}{2}\,|\,\alpha\,|^2-\tfrac{1}{2}\,|\,\beta\,|^2)\,, \quad (4.6)$$

$$|\,\langle\alpha\,|\,\beta\rangle\,|^2=\exp(-\,|\,\alpha-\beta\,|^2)\,. \quad (4.7)$$

In spite of its overcompleteness, the coherent states form a natural basis. We can expand an arbitrary state $\langle\psi|$ (or $|\psi\rangle$) in terms of $\langle\alpha|$ (or $|\alpha\rangle$) as

$$\frac{1}{\pi}\int d^2\alpha\,|\alpha\rangle\langle\alpha\,|=I\,, \quad (4.8)$$

$$\langle\psi\,|=\frac{1}{\pi}\int d^2\alpha\langle\psi\,|\,\alpha\rangle\langle\alpha\,|\,, \quad (4.9a)$$

$$|\psi\rangle=\frac{1}{\pi}\int d^2\alpha\,|\alpha\rangle\langle\alpha\,|\,\psi\rangle\,, \quad (4.9b)$$

where

$$\langle\psi\,|\,\alpha\rangle\equiv e^{-|\alpha|^2/2}f(\alpha)\,, \quad (4.10)$$

$$d^2\alpha\equiv d\alpha_1 d\alpha_2\,, \quad (4.11)$$

and $f(\alpha)$ is an analytic function of $\alpha\equiv\alpha_1+i\alpha_2$. Of course, the physical amplitude is $\langle\psi\,|\,\alpha\rangle$, not $f(\alpha)$.

In our model, we encounter a periodic q. The momentum operator produces only discrete eigenstates. We shall modify the coherent-state basis to take this periodic boundary condition into account. We need to modify Eqs. (4.5) and (4.8) to

$$\langle q \mid \alpha\rangle = \sum_{n=-\infty}^{\infty} \left[\frac{\omega}{\pi\hbar}\right]^{1/4} e^{-|\alpha|^2/2+\alpha^2/2} \times \exp\{-[\sqrt{\omega/2\hbar}(q+n)-\alpha]^2\} , \quad (4.12)$$

$$\langle m \mid \alpha\rangle = \left[\frac{4\pi\hbar}{\omega}\right]^{1/4} e^{-|\alpha|^2/2-\alpha^2/2} \times \exp\left\{-\left|\left[\frac{2\pi^2\hbar}{\omega}\right]^{1/2} m + i\alpha\right|^2\right\} , \quad (4.13)$$

$$\frac{1}{\pi}\int_0^{(\omega/2\hbar)^{1/2}} d\alpha_1 \int_{-\infty}^{\infty} d\alpha_2 \mid \alpha\rangle\langle\alpha \mid = I , \quad (4.14)$$

where the momentum eigenvalue in (4.12) is

$$p = 2\pi\hbar m . \quad (4.15)$$

The periodicity in q implies that we only need to integrate α_1 in (4.13) from 0 to $\sqrt{\omega/2\hbar}$.

The coherent-state amplitude for an arbitrary state $\langle\psi\mid$ is

$$\langle\psi \mid \alpha\rangle = \sum_m \langle\psi \mid m\rangle\langle m \mid \alpha\rangle , \quad (4.16)$$

where

$$\psi_m \equiv \langle m \mid \psi\rangle \quad (4.17)$$

is the momentum state wave function.

In Sec. VI, we shall plot some typical $|\langle\psi\mid\alpha\rangle|^2$ as a function of

$$q' \equiv \sqrt{2\hbar/\omega}\,\alpha_1 \text{ and } p' \equiv \sqrt{2\hbar\omega}\,\alpha_2 , \quad (4.18)$$

where q' and p' are analogs of classical q and p.

Under the resonance condition described in (3.4),

$$2\pi\hbar = M/N , \quad (4.19)$$

with NM = even, the eigenstate wave function obeys

$$\phi_{m+N} = e^{-ia}\phi_m . \quad (4.20)$$

It is straightforward to show that

$$\langle m+N \mid \alpha + iM/\sqrt{2\hbar\omega}\rangle = e^{-i\alpha_1 M/\sqrt{2\hbar\omega}}\langle m \mid \alpha\rangle . \quad (4.21)$$

Substituting (4.19) and (4.20) into (4.15), we have

$$\begin{aligned}\langle\phi \mid \alpha + iM/\sqrt{2\hbar\omega}\rangle &= \sum_m \langle\phi \mid m+N\rangle\langle m+N \mid \alpha + iM/\sqrt{2\hbar\omega}\rangle \\ &= \sum \langle\phi \mid m\rangle e^{ia} e^{-i\alpha_1 M/\sqrt{2\hbar\omega}}\langle m \mid \alpha\rangle \\ &= e^{i(a-\alpha_1 M/\sqrt{2\hbar\omega})}\langle\phi \mid \alpha\rangle . \end{aligned} \quad (4.22)$$

Hence, for an eigenstate $\langle\phi\mid$, we have

$$|\langle\phi \mid \alpha + iM/\sqrt{2\hbar\omega}\rangle|^2 = |\langle\phi \mid \alpha\rangle|^2 . \quad (4.23)$$

Note that the displacement $\alpha \to \alpha + iM/\sqrt{2\hbar\omega}$ corresponds to

$$q' \to q' , \quad (4.24a)$$

$$p' \to p' + M . \quad (4.24b)$$

Thus for $2\pi\hbar = M/N$ with even NM, the coherent-state graph of $|\langle\phi\mid\alpha\rangle|^2$ for an eigenstate $\langle\phi\mid$ is periodic in p' with period M. In particular, for $2\pi\hbar = 1/N$ ($M=1$), the coherent state graph of $|\langle\phi\mid\alpha\rangle|^2$ is periodic in both q' and p' with period 1.

B. Wigner functions and coarse-grained Wigner functions

It has been suggested that Wigner functions play an important role in the correspondence between a quantum and a classical system.[11,12] We wish to point out that $|\langle\psi\mid\alpha\rangle|^2$ in the coherent-state representation is a coarse-grained Wigner function. The process of coarse graining[20] appears to be necessary to obtain a smooth quantum to classical transition.[14]

The Wigner function for a quantum state $|\psi\rangle$ may be defined from its q-space wave function via

$$\begin{aligned}\psi_W(q,p) &\equiv \frac{1}{\sqrt{2\pi\hbar}}\int dx \exp\left[-\frac{i}{\hbar}p\cdot x\right] \times \langle q + x/2 \mid \psi\rangle\langle\psi \mid q - x/2\rangle \\ &= \frac{1}{\sqrt{2\pi\hbar}}\int dx \exp\left[\frac{i}{\hbar}p\cdot x\right] \times \langle q - x/2 \mid \psi\rangle\langle\psi \mid q + x/2\rangle . \end{aligned} \quad (4.25)$$

It is easy to see that ψ_W is always real. The Wigner function contains both parameters p and q, which provides a natural association with the classical system. We can also express the Wigner function in terms of the momentum-space wave function, and obtain a similar expression.

We cannot directly interpret ψ_W as a probability distribution. Even though ψ_W is real, it is not always positive. Indeed, if the original wave function is localized in x, the Wigner function is oscillatory in sign. We wish to have an alternative expression which is both positive-definite and having a proper classical limit. A properly coarse-grained Wigner function appears to be the solution.

To introduce the coarse graining, we need to consider two Wigner functions ψ_W and ϕ_W with

$$\phi_W(q,p) \equiv \frac{1}{\sqrt{2\pi\hbar}}\int dx \exp\left[\frac{i}{\hbar}p\cdot x\right] \times \langle q - x/2 \mid \phi\rangle\langle\phi \mid q + x/2\rangle . \quad (4.26)$$

Then, it is easy to show that

$$\int dp\,dq\,\psi_W(q,p)\phi_W(q,p)$$
$$=\frac{1}{2\pi\hbar}\int dx\,dx'\,dp\,dq\,e^{-(i/\hbar)p\cdot(x-x')}\langle q+x/2\,|\,\psi\rangle\langle\psi\,|\,q-x/2\rangle\langle q-x'/2\,|\,\phi\rangle\langle\phi\,|\,q+x'/2\rangle$$
$$=\frac{1}{2\pi\hbar}\int dx\,dx'\,dq\,2\pi\hbar\delta(x-x')\langle q+x/2\,|\,\psi\rangle\langle\psi\,|\,q-x/2\rangle\langle q-x'/2\,|\,\phi\rangle\langle\phi\,|\,q+x'/2\rangle$$
$$=\int dx\,dq\langle q+x/2\,|\,\psi\rangle\langle\psi\,|\,q-x/2\rangle\langle q-x/2\,|\,\phi\rangle\langle\phi\,|\,q+x/2\rangle\ . \tag{4.27}$$

In terms of

$$\xi=q+x/2,\quad \eta=q-x/2\ , \tag{4.28}$$

we obtain

$$\int dp\,dq\,\psi_W(q,p)\phi_W(q,p)$$
$$=\int d\xi\,d\eta\langle\phi\,|\,\xi\rangle\langle\xi\,|\,\psi\rangle\langle\psi\,|\,\eta\rangle\langle\eta\,|\,\phi\rangle$$
$$=|\langle\phi\,|\,\psi\rangle|^2\ , \tag{4.29}$$

which is always positive. If we choose ψ as a physical state localized at (p',q'), then, we call (4.29) a coarse-grained Wigner function. It describes a Wigner function ϕ_W coarse grained by the state ψ. We shall use (p',q') as its new momentum and coordinate labels.

In this paper, we choose the localized state ψ_α as the coherent state centered at (p',q'). The position-space wave functions are given in (4.5a) and (4.12). The relation between p',q' and α_1,α_2 are described by (4.18). The coarse-grained Wigner function of any $|\phi\rangle$ by the coherent state ψ_α is precisely the coherent-state amplitude squared, $|\langle\phi\,|\,\alpha\rangle|^2$, described in Sec. IV A.

V. NUMERICAL RESULTS

In this section, we study the eigenstates associated with the quantum Chirikov map for rational $2\pi\hbar$. We begin with a quick review of the classical Chirikov map. We then present the results of pseudoenergies and eigenstates for the quantum system. We describe the eigenstates in the coherent-state representation.

A. Classical Chirikov map

The classical Chirikov map is described by

$$p_{n+1}=p_n+\frac{k}{2\pi}\sin(2\pi q_n)\ , \tag{5.1}$$

$$q_{n+1}=q_n+p_{n+1}(\mathrm{mod}\ 1)\ . \tag{5.2}$$

This map has been studied thoroughly by Chirikov, Greene, and others.[1] We refer the readers to the above references for details. We wish to point out a few important features relevant to our discussions.

(i) For $k=0$, the nature of the orbit is determined completely by p. If $p=M/N$ is a rational number with M and N being relatively prime, then, any initial point (p,q) leads to an N cycle under iterations. If p is an irrational number, then, any initial point (p,q) leads to a continuous horizontal line. [See Fig. 3(a).]

(ii) For $k\neq 0$, we introduce a winding number w of an N-cycle orbit as follows: First we ignore temporarily (mod 1) in Eq. (5.2) and let q vary from $-\infty$ to ∞. If during N iterations the value of q changes by M, then, we define the winding number $w=M/N$, a rational. We define an orbit with an irrational winding number as the limit of a sequence of orbits with rational winding numbers. For most fixed irrational numbers and for a sufficiently small k, KAM theorem tells us that such an orbit exists in the form of a continuous curve. This curve wraps around the q direction and is known as a horizontal KAM curve. If we iterate a point on this KAM curve N times, and denote q_N-q_0 as M, the ratio M/N approaches the given irrational number as $N\to\infty$. [See Fig. 3(b).]

(iii) As the control parameter k in Eq. (5.1) increases, many of the horizontal KAM curves disappear. At $k=k_c=0.971\,635\ldots$, the last horizontal KAM curves begin to disappear. These last KAM curves have the winding numbers

$$w_1=\frac{\sqrt{5}-1}{2}=0.618\,034 \tag{5.3a}$$

and

$$w_2=1-w_1=0.381\,966\ . \tag{5.3b}$$

For $k<k_c$, the momentum p is bounded by these KAM curves, and cannot change by more than one under any number of iterations. However, for $k>k_c$, p can increase or decrease indefinitely. [See Fig. 3(c).]

(iv) There are additional cycles and KAM curves around elliptical fixed points and cycles such as $p=0$, $q=\frac{1}{2}$, and $p=\frac{1}{2}$, $q=0$, and $\frac{1}{2}$. These KAM curves persist beyond k_c. However, at sufficiently large k, most of these KAM curves also disappear. The iteration of a single point can generate points all over the pq plane. [See Figs. 3(d)–3(f).]

B. Pseudoenergies

We consider the quantum Chirikov map with a rational $2\pi\hbar$,

$$2\pi\hbar=M/N\ . \tag{5.4}$$

We choose $NM=$even. The $N\times N$ matrix is given in (3.24),

$$U(a)_{ss'}=\frac{1}{N}\exp[-i2\pi^2s^2\hbar+i(s'-s)a/N]$$
$$\times\sum_{j=1}^{N}\exp\{i2\pi(s'-s)j/N-iz\cos[(2\pi j+a)/N]\}, \tag{5.5}$$

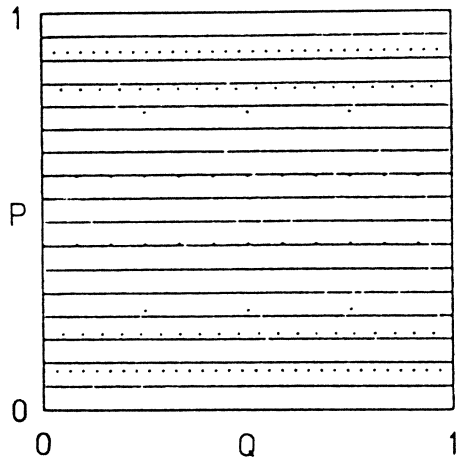

(a)

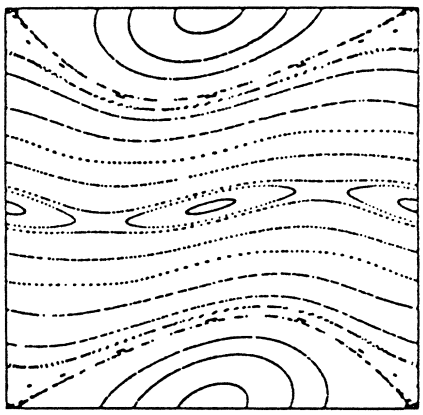

(b)

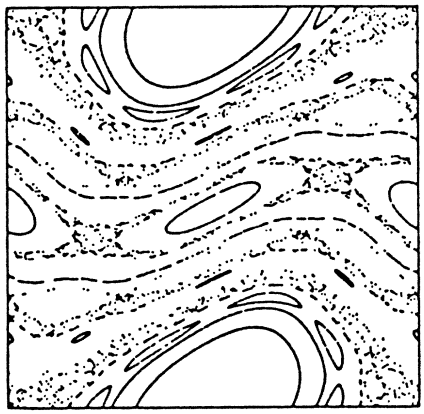

(c)

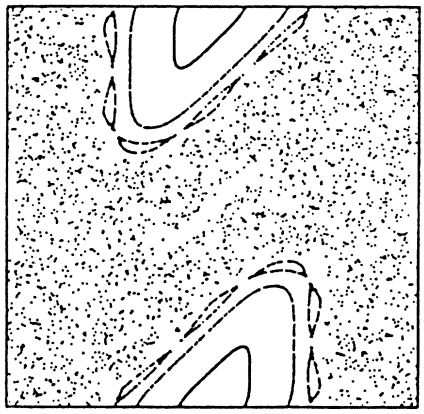

(d)

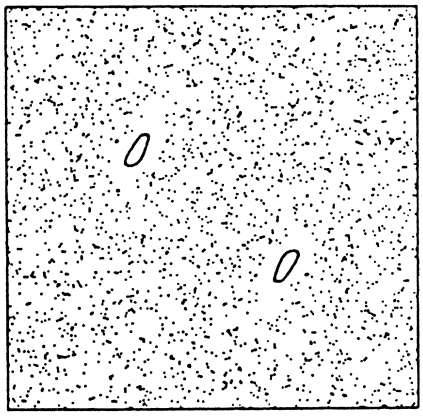

(e)

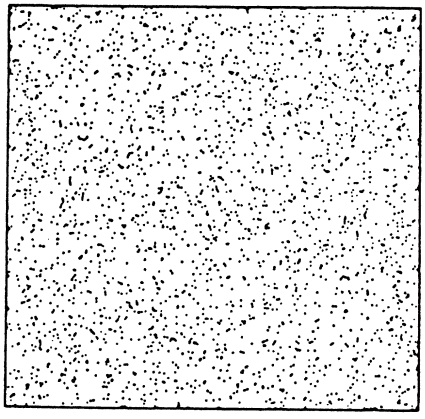

(f)

FIG. 3. The invariant trajectories generated by the iterations of Chirikov map from a small number of initial points. These graphs all plotted in the region $0 \leq q \leq 1$, $0 \leq p \leq 1$. If $p > 1$, we plot $[q, p(\text{mod } 1)]$. The parameter k associated with these graphs are (a) $k = 0$, (b) $k = 0.5$, (c) $k = 1$, (d) $k = 2$, (e) $k = 5$, and (f) $k = 10$. Several initial points are needed to generate (c). However, a single point is sufficient to produce (f).

with

$$z = k/(4\pi^2\hbar) . \tag{5.6}$$

For simple cases such as $N=2$ or 4, we can find the eigenvalues analytically. However, for a large N, this is not always feasible. We only present the numerical results here.

The eigenvalues of $U(a)$ are of the form $e^{-i\omega(a)}$ where $\omega(a)$ is the pseudoenergy. For $2\pi\hbar = M/N$, there are N eigenvalues for each a. The variation of ω as a function of a gives rise to the energy band. In Fig. 4, we plot ω's as functions of a for a fixed $2\pi\hbar = \frac{1}{8}$, but for several different values of k. At $k \leq 1$ [Fig. 4(a)], there are practically no a dependences. At $k=5$ [Fig. 4(b)], there are significant a dependences which lead to a (barely) nonoverlapping band structure. At $k=10$ [Fig. 4(c)], the bands definitely overlap.

In Fig. 5, we illustrate how the pseudoenergies ω vary as functions of a for equivalent fractions. All graphs in Fig. 5 have $k=10$ and the same $2\pi\hbar$ represented by different reducible fractions. In graphs (a), (b), and (c), they are represented by $(2\pi\hbar =)\ \frac{1}{2}$, $\frac{2}{4}$, and $\frac{3}{6}$. We can obtain Figs. 5(b) and 5(c) from 5(a) by cutting the graph 5(a) into two or three parts, and then overlay these parts on top of each other. These graphs always give the same band structure.

In Fig. 6, we plot the pseudoenergies as functions of k for $2\pi\hbar = \frac{1}{8}$, and for $a=0$ and 0.382. At $a=0$ [Fig. 6(a)], the parity is a good quantum number. The trajectories with different parity can cross each other. However, for $a=0.382$, no such crossings are observed.[21]

In Fig. 7, we illustrate the pseudoenergies as functions of a (band structures) for $2\pi\hbar$ being several of the Fibonacci ratios, $\frac{1}{2}, \frac{2}{3}, \frac{5}{8}, \frac{8}{13}$. We have chosen not to plot

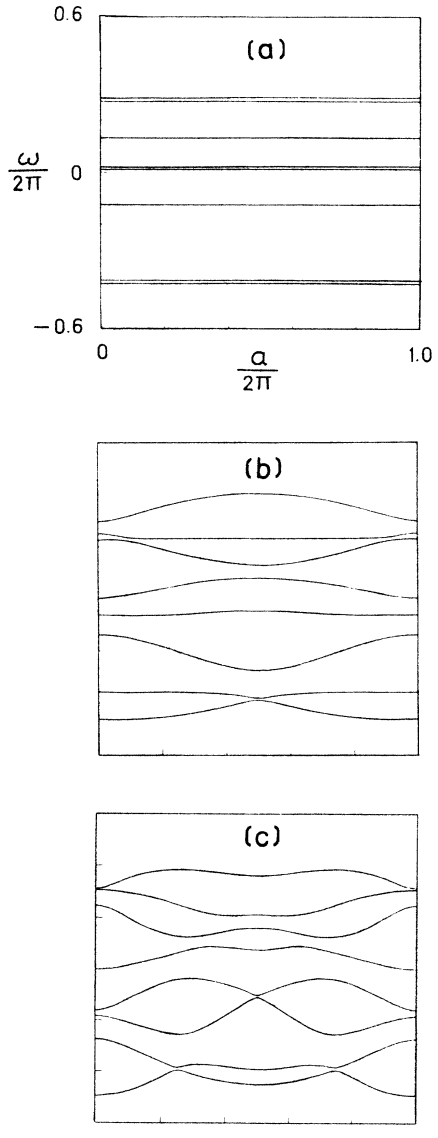

FIG. 4. Pseudoenergies as functions of a for $2\pi\hbar = \frac{1}{8}$, and for several values of k. The parameters used are (a) $k=1$, (b) $k=5$, and (c) $k=10$.

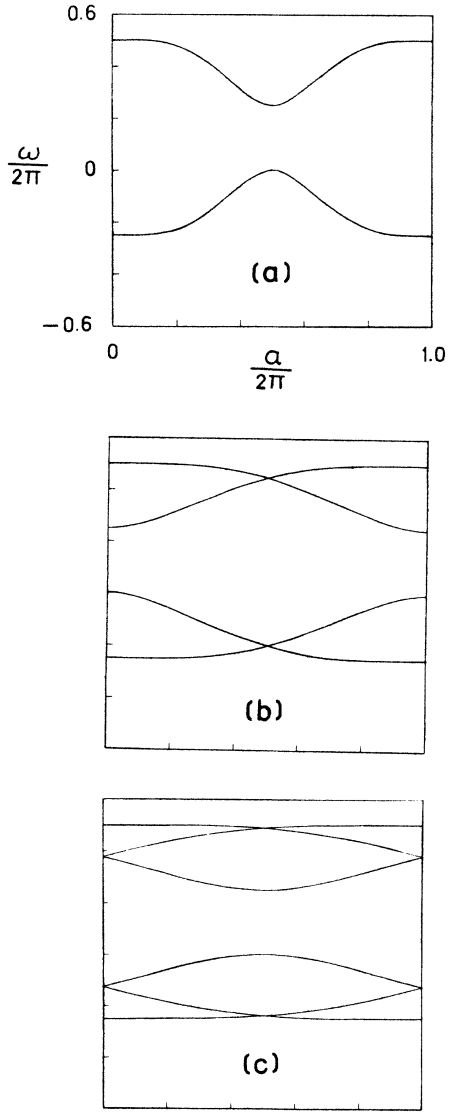

FIG. 5. Pseudoenergies as functions of parameter a for $k=10$, and for different fractional representations of $2\pi\hbar$. These fractions are (a) $\frac{1}{2}$, (b) $\frac{2}{4}$, and (c) $\frac{3}{6}$.

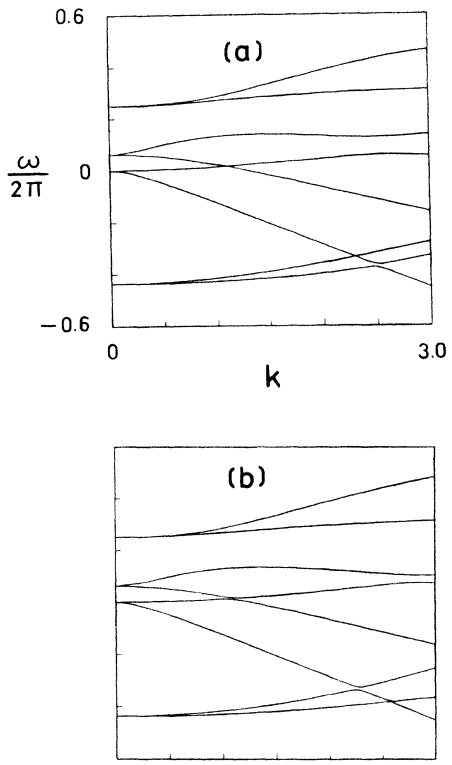

FIG. 6. Pseudoenergies as functions of k for $2\pi\hbar=\frac{1}{8}$ and $a=0$ and 0.382. (a) $a=0$. Parity is a good quantum number. Energy levels of states with different parity can cross each other, but those of states with same parity repel each other. (b) $a=0.382$. Parity is no longer a good quantum number. All energy levels repel each other and no crossings are observed.

the graph associated with $\frac{3}{5}$ because $\frac{3}{5}$ is an odd/odd fraction. This odd fraction leads to 10 bands ($\frac{3}{5}=\frac{6}{10}$) which does not fit in well with the other fractions. As we can see, as the number of bands increase, the widths of each band go to zero rapidly as we approach the golden ratio. Even though the numerical values of $2\pi\hbar$ have not changed much, the band width changes drastically depending on whether it can be represented by a simple ratio or not. A large width is always associated with a simple ratio. This feature is very similar to that of the solvable model discussed in Refs. 7 and 8.

There are indications that the energy spectrum for a certain irrational $2\pi\hbar$ may form a Cantor set. First, Grempel and Prange showed that a quantum Chirikov map is equivalent to a one-dimensional tight-binding model.[7] For an irrational $2\pi\hbar$, this leads to an almost-periodic tight-binding system. For certain simple classes of such models, there are rigorous results that the spectrum must contain a Cantor set.[22] Unfortunately, the generalized quantum Chirikov map does not fall into the category specified in Ref. 22. In a companion paper, we shall investigate this problem and its implications more thoroughly.[13]

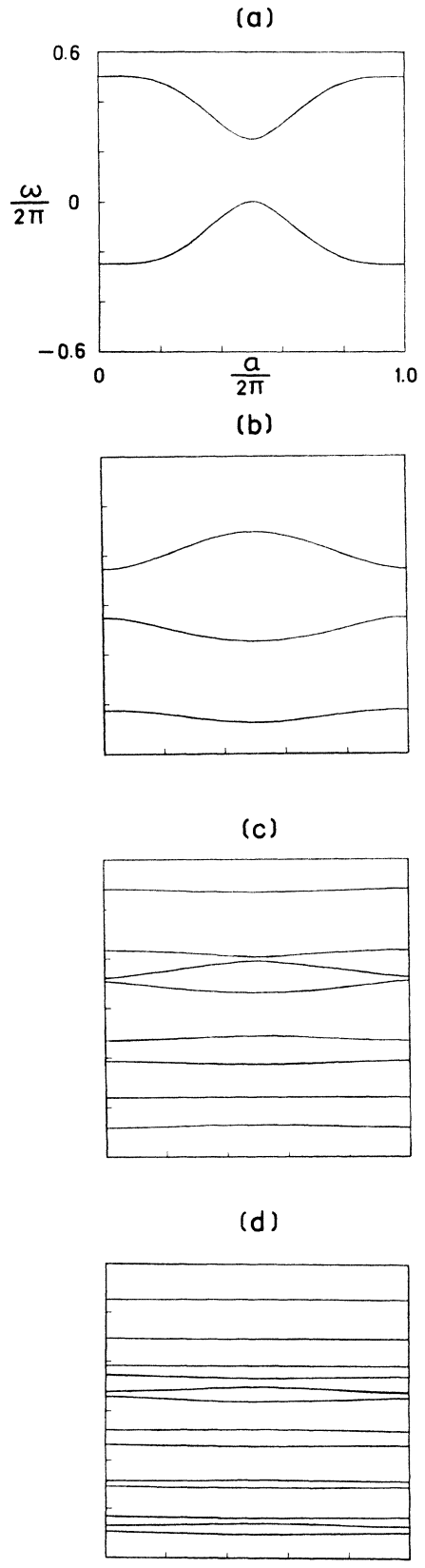

FIG. 7. The pseudoenergies as functions of a for $k=10$ and for $2\pi\hbar$ being the Fibonacci ratios (a) $\frac{1}{2}$, (b) $\frac{2}{3}$, (c) $\frac{5}{8}$, and (d) $\frac{8}{13}$. The odd/odd ratio $\frac{3}{5}$ does not fit well with the rest, and has not been included here.

C. Coherent-state pictures

Using (4.15) and (4.16), we can express any state in the coherent-state representation. As we have shown in Sec. IV and in the Appendix, when $(2\pi\hbar)^{-1}$ is an even integer, the coherent-state amplitude squared, $|\langle\phi|\alpha\rangle|^2$, for an eigenstate $\langle\phi|$ is periodic in p with periodicity 1. When $(2\pi\hbar)^{-1}$ is an odd integer, the period in p is 2. For the general case $2\pi\hbar=M/N$, the periodicity is M when MN is even, and $2M$ when MN is odd. In this section, we concentrate on the simple case when $(2\pi\hbar)^{-1}$ is an integer.

As discussed in Sec. IV, the coherent-state representation is a coarsely-grained Wigner function. We first begin with a Wigner function without coarse graining. In Fig. 8(a), we plot the Wigner function for a eigenstate at $(2\pi\hbar)^{-1}=10$. This eigenstate corresponds to the classical fixed point at $(p=0,\ q=\frac{1}{2})$. Because of the periodicity in p and q, the Wigner function is represented by $2N\times 2N$ δ functions. The coefficients of these δ functions can be both positive and negative. If we increase N, we encounter more δ functions which do not make it any smoother.

In Fig. 8(b), we plot the same eigenstate in the coherent-state representation. This is equivalent to averaging the δ functions in Fig. 8(a) by Gaussians. Note that the δ functions in the center region and in the four corners of Fig. 8(a) have alternative signs on even and odd lattice sites. They are practically averaged out to zero in Fig. 8(b). Only those regions of Fig. 8(a) whose δ functions on even and odd sites have the same sign contribute. As we increase N, we arrive at a structure which is very close to a classical invariant orbit. In other words, coarse grainings are crucial for achieving smoother transitions to classical results.[14,23]

In Fig. 9 we compare analogous eigenstates with the same $k=1$ and $2\pi\hbar=\frac{1}{34}$, but with different a. We find that their coherent-state pictures are practically indistinguishable. As we increase N, the distinction in different a becomes even smaller.

For an odd integer N, we expect the coherent-state graph has a period 2 in p. We plot a few eigenstates in Fig. 10 to illustrate this behavior. For $2\pi\hbar=M/N$, the natural periodicity of the eigenstate is M in variable p if NM is even, and is $2M$ in variable p if MN is odd. In Figs. 10(a) and 10(b), $2\pi\hbar=\frac{2}{68}=\frac{1}{34}$, the natural periodicity in p is 1. Thus, we see the repetition as p varies from 0 to 2. In Figs. 10(c) and 10(d), $2\pi\hbar=\frac{2}{69}$, the natural periodicity in p is 2. In Figs. 10(e) and 10(f), we have $2\pi\hbar=\frac{2}{70}=\frac{1}{35}$. Since both 1 and 35 are odd numbers, the natural periodicity of the eigenstate is again 2, as shown

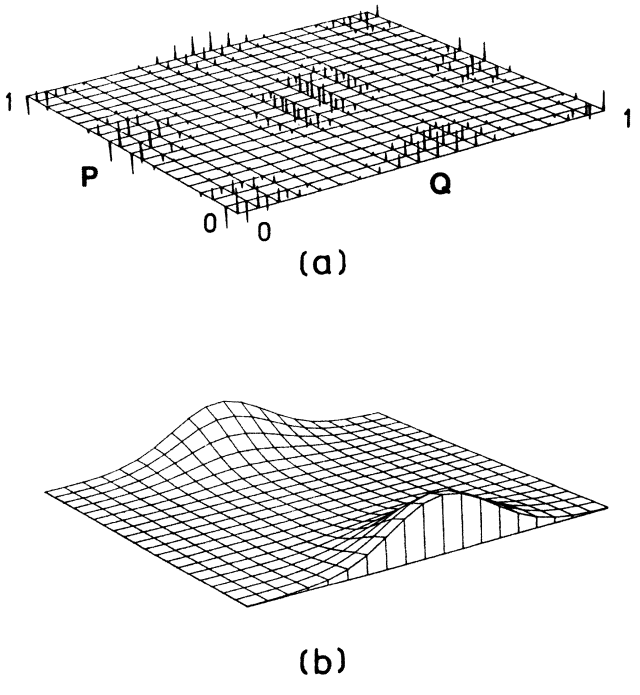

FIG. 8. Wigner functions and the coarsely-grained Wigner function for an eigenstate with $k=1$, $2\pi\hbar=\frac{1}{10}$, $a=0$. (a) The full Wigner function with spikes representing δ functions. (b) After coarse-graining the Wigner function in (a), we obtain this coherent-state $|\psi|^2$ picture.

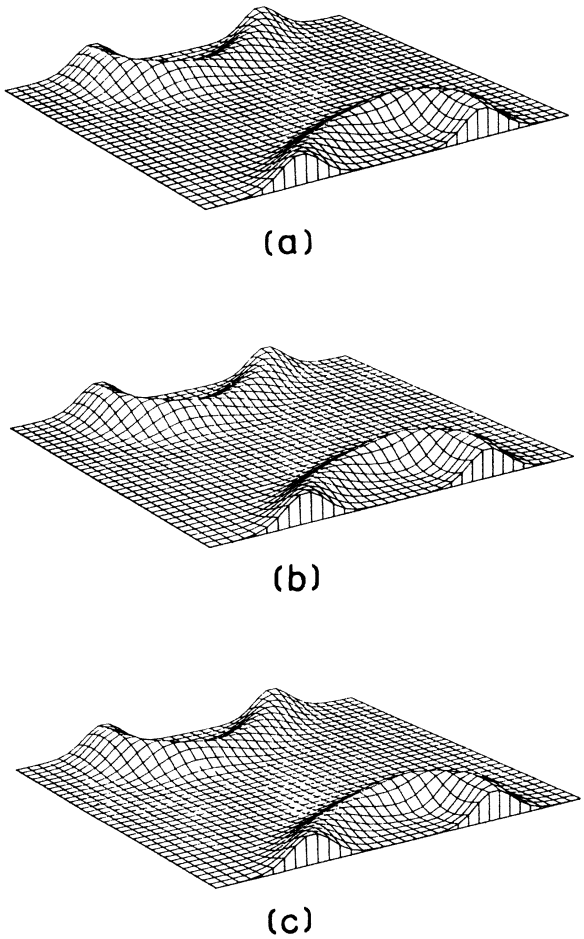

FIG. 9. The a dependence as appeared in the quantum eigenstates $|\psi|^2$ in the coherent-state representation. The parameters used are $k=1$, $2\pi\hbar=\frac{1}{34}$, and (a) $a=0$, (b) $a=0.372$, and (c) $a=0.5$.

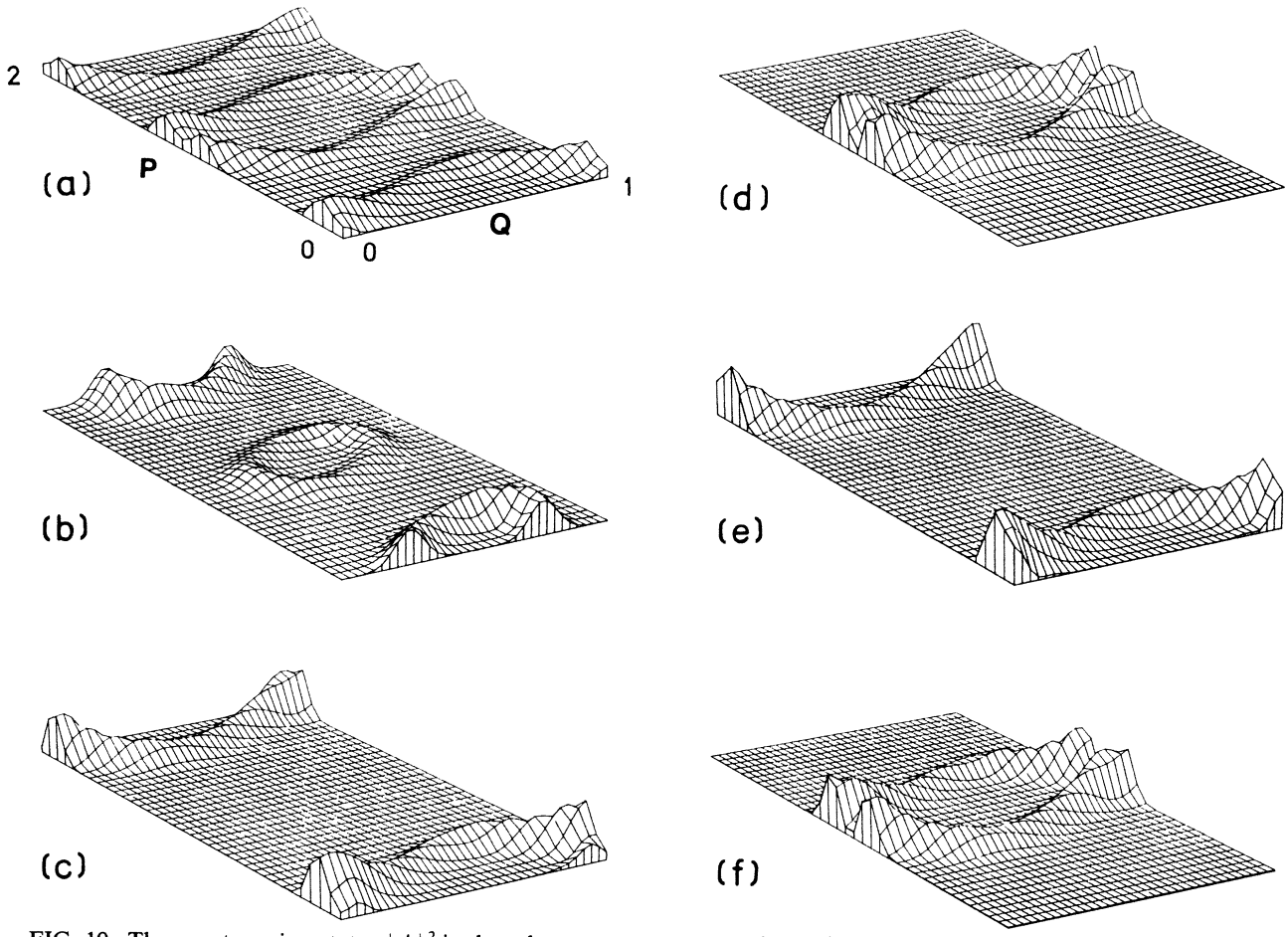

FIG. 10. The quantum eigenstates $|\psi|^2$ in the coherent-state representation. The parameters used are $k=1$, $a=0$, and (a) and (b) $2\pi\hbar=\frac{2}{68}$, (c) and (d) $2\pi\hbar=\frac{2}{69}$, and (e) and (f) $2\pi\hbar=\frac{2}{70}$.

in Figs. 10(e) and 10(f). In Fig. 11, we choose $k=1$ and $(2\pi\hbar)^{-1}=N=102$, and plot several eigenstates in the coherent-state representation. By comparing Fig. 11 with the classical map Fig. 3(c), we can identify clearly each of these quantum states with the classical analog. In particular, the classical cycles are represented in the quantum map by isolated peaks of width $\sqrt{\hbar/2}=1/\sqrt{4\pi N}$ and the KAM curves are represented in the quantum map by walls with width $1/\sqrt{4\pi N}$. The chaotic regions are represented in the quantum map by ripples which no longer have well-defined wall structure. To see the qualitative transition in quantum maps from a KAM region to a chaotic region, we vary k from $k=0$ to $k=10$ in Fig. 12. In Figs. 12(a) and 12(b) ($k=0$ and 1), we see well-defined KAM walls. In Fig. 12(c) ($k=5$), we encounter an eigenstate which has no well-defined peaks or walls. In Fig. 12(d) ($k=10$), we arrive at a quantum map whose classical map [Fig. 3(f)] is chaotic. Both Figs. 12(c) and 12(d) look similar to snapshots of ocean waves.

To conclude this section, we include the coherent-state pictures for states with different $2\pi\hbar$'s. Figures 13(a)–13(c) and 11(b) describe the quantum analogs of the same classical KAM curve. All these states describe quantum KAM walls with widths $\sim O(\sqrt{\hbar/2})$.

VI. DISCUSSIONS

In this paper, we develop a coherent-state method for analyzing a resonance quantum map. In a separate paper, we shall consider the real time evolution of states initially localized in both p and q. We shall illustrate the effect of KAM curves on the propagation of these states.

We have seen in Sec. III that the quantum resonance in the Chirikov map follows from a classical-resonance condition. It is important to know whether this correspondence is a general feature of the quantum resonance or not. In deriving the classical Chirikov map from a periodically kicked rotor, if the kicks have a small but finite duration, we arrive at a slightly modified iterative system. The modified system is no longer invariant under the (resonance) symmetry $p\rightarrow p+1$. If a classical resonance is indeed a prerequisite of a quantum resonance, then, the quantum resonance will be a rare phenomena.

Another related and active research area is quantum chaos.[6] At the moment, there are no generally accepted definitions of quantum chaos, but there are many indications of quantum-chaotic phenomena.[24] One important indication of quantum chaos is the energy-level distribution. It has been suggested that the spectral statistics of

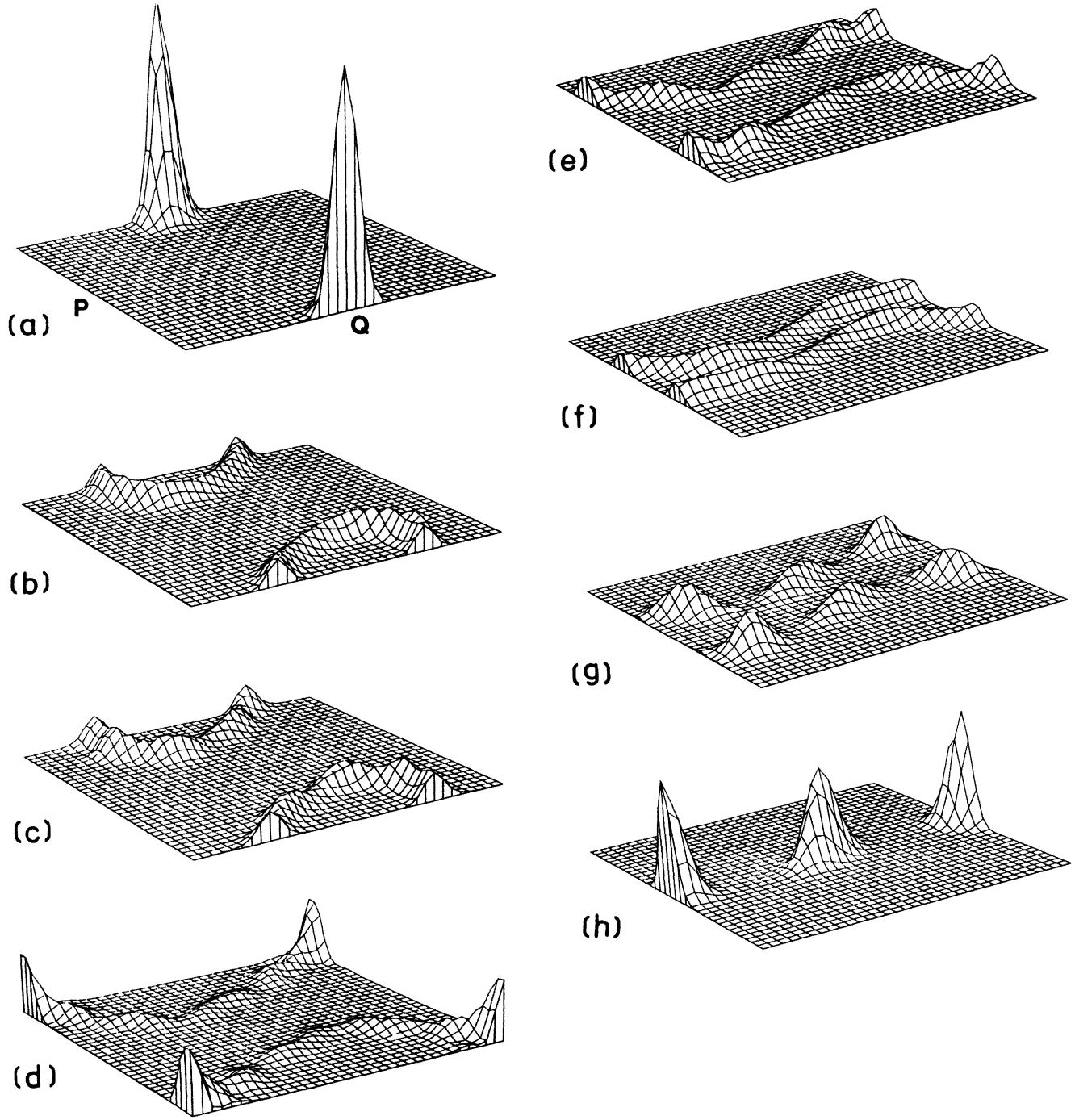

FIG. 11. The quantum eigenstate $|\psi|^2$ in the coherent-state representation. Each of the eigenstates is closely related to a KAM curve or other classical orbits generated by appropriate initial points in Fig. 3(c). The parameters used are $k=1$, $2\pi\hbar=\frac{1}{102}$, and $a=0$.

the quantum system are related to the stochasticity of a classical system. In particular, the level fluctuations of a chaotic quantum system may follow that of the Gaussian ensemble of random matrices.[21] This random matrix description also leads to the avoided level crossings (level repulsions) as one varies the interaction strength. Recently, Izrailev studied extensively the quasienergy level statistics for quantum Chirikov map.[25] At $k=0$, the level distribution obeys Poisson distribution which describes an independent level distribution. For very large k, the level distribution indeed resembles that of Gaussian ensemble of random unitary matrices. Other indications of quantum chaos include nonvanishing of quantum Kolmogorov entropy, erratic nodal pattern, and vanishing of spatial

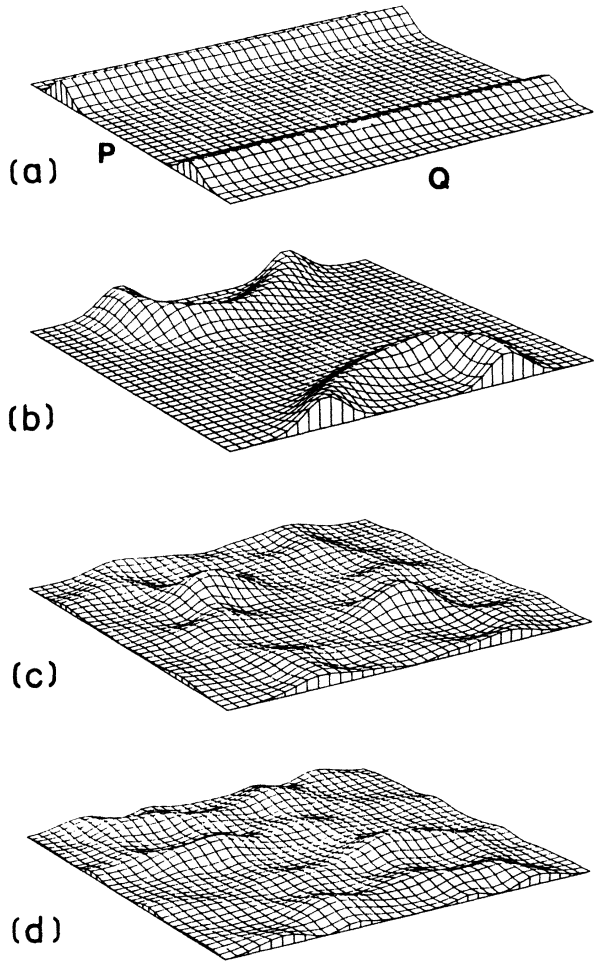

FIG. 12. The k dependence as appeared in the selected quantum eigenstates $|\psi|^2$ in the coherent-state representation. Parameters used are $2\pi\hbar=\frac{1}{34}$, $a=0$. The parameter k varies from (a) $k=0$, (b) $k=1$, (c) $k=5$, and finally to (d) $k=10$. Classically, the system is integrable at $k=0$, and appears to be completely chaotic at $k=10$.

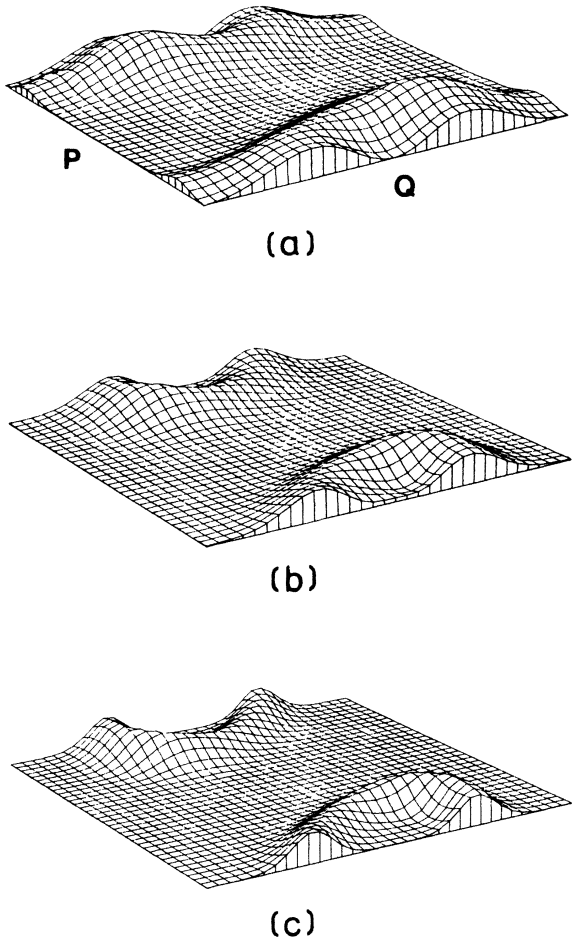

FIG. 13. The $2\pi\hbar$ dependence of quantum eigenstate $|\psi|^2$ as appeared in the coherent-state picture. We fix the parameters $k=1$, $a=0$, and vary $2\pi\hbar$ from (a) $2\pi\hbar=\frac{1}{8}$, (b) $2\pi\hbar=\frac{1}{16}$, to (c) $2\pi\hbar=\frac{1}{34}$. Figure 11(b) describes a similar picture with $2\pi\hbar=\frac{1}{102}$.

correlation function.[26] Our approach offers a different prospect of quantum chaos.

ACKNOWLEDGMENTS

We wish to thank Professor A. Jackson, Professor Y. Oono, and Professor R. Schult for stimulating discussions. We are grateful to Professor G. Casati for many helpful suggestions, and for bringing their rigorous result on nonrecurrent quantum behavior to our attention. We thank the Research Board of the University of Illinois for providing us with some free computer time. This work was supported in part by the National Science Foundation under Grant No. PHY-82-01948.

APPENDIX: $2\pi\hbar$ AS A REDUCIBLE FRACTION

In this appendix we consider $2\pi\hbar$ as a reducible fraction. One reason for studying a reducible fraction is to consider

$$2\pi\hbar=M/N \tag{A1}$$

when both M and N are odd. Then, we have from Eq. (3.6) in Sec. III,

$$U_{m+N,m'+N}=-U_{m,m'}\ , \tag{A2}$$

which implies

$$U_{m+2N,m'+2N}=U_{m,m'}\ . \tag{A3}$$

In other words, $U_{mm'}$ is periodic in indices (m,m') with period $2N$. This is equivalent to study a reducible fraction

$$2\pi\hbar=2M/(2N)\ , \tag{A4}$$

where $2M$ and $2N$ are even. Another reason for studying reducible $2\pi\hbar$ is for analyzing an irrational $2\pi\hbar$. We approximate an irrational $2\pi\hbar$ as a sequence of rationals. It is very important to see how the reducibility of the rationals affects the behavior of the system.

We consider the general situation

$$2\pi\hbar = nM/(nN) , \tag{A5}$$

where M/N is irreducible, and n is an integer common factor. We begin with the simple case of $n=2$, $MN=$odd.

1. $n=2$, $MN=$odd

In analogy to (3.11), we construct from $U_{mm'}$ a set of $2N\times 2N$ unitary matrices $U(a)_{ss'}$, $1\le s,s'\le 2N$, as follows:

$$U(a)_{ss'} = \sum_{l=-\infty}^{\infty} U_{s,s'+2Nl} e^{-2ial} . \tag{A6}$$

Note that we have chosen the phase in (A6) as e^{-2ial} From (A2) and (A6), we obtain

$$U_{s+N,s'+N} = -U_{ss'} , \tag{A7}$$

$$U_{s+N,s'} = -e^{-2ia} U_{s,s'+N} \tag{A8}$$

for $1\le s,s'\le N$. We can express these $2N\times 2N$ matrices in terms of block matrices as

$$U(a) = \begin{bmatrix} u_1 & e^{ia}u_2 \\ -e^{-ia}u_2 & -u_1 \end{bmatrix} , \tag{A9}$$

where u_1 and u_2 are $N\times N$ matrices. The unitary condition

$$U^{\dagger}(a)U(a) = \begin{bmatrix} I & 0 \\ 0 & I \end{bmatrix} , \tag{A10}$$

leads to

$$u_1^{\dagger}u_1 + u_2^{\dagger}u_2 = I , \tag{A11a}$$

$$u_1^{\dagger}u_2 + u_2^{\dagger}u_1 = 0 . \tag{A11b}$$

Equation (A9) implies that both

$$u_+ \equiv u_1 + u_2 \tag{A12a}$$

and

$$u_- \equiv u_1 - u_2 \tag{A12b}$$

are $N\times N$ unitary matrices. We also decompose the $2N$-component eigenvector $\phi(a)_s$, $1\le s\le 2N$, as the direct sum of two N-component vectors ϕ_1 and $e^{-ia}\phi_2$,

$$\phi(a) = \begin{bmatrix} \phi_1 \\ e^{-ia}\phi_2 \end{bmatrix} . \tag{A13}$$

The eigenequation

$$U(a)\phi(a) = e^{-i\omega(a)}\phi(a) \tag{A14}$$

leads to

$$u_1\phi_1 + u_2\phi_2 = e^{-i\omega}\phi_1 , \tag{A15a}$$

$$-u_2\phi_1 - u_1\phi_2 = e^{-i\omega}\phi_2 . \tag{A15b}$$

From ϕ_1 and ϕ_2, we can construct

$$\phi_{\pm} \equiv \phi_1 \pm \phi_2 . \tag{A16}$$

It is straightforward to show that $\phi_{\pm}$ are eigenstates of the $N\times N$ unitary matrices u_-u_+ and u_+u_-,

$$(u_-u_+)\phi_+ = e^{-2i\omega}\phi_+ , \tag{A17a}$$

$$(u_+u_-)\phi_- = e^{-2i\omega}\phi_- . \tag{A17b}$$

The converse is also true. From the $N\times N$ unitary matrices u_-u_+ and u_+u_-, we can construct via (A17) the eigenvalues $e^{-2i\omega(a)}$ and the eigenvectors $\phi_{\pm}$. From these $\phi_{\pm}$, we can construct $\phi(a)_s$ and consequently eigensolutions to the original $\infty\times\infty$ unitary matrix $U_{mm'}$. Note that ϕ_+ and ϕ_- are simply related by

$$u_+\phi_+ = e^{-i\omega}\phi_- , \tag{A18a}$$

$$u_-\phi_- = e^{-i\omega}\phi_+ . \tag{A18b}$$

As mentioned in Sec. IV, another important consequence of $2\pi\hbar = M/N$ with odd M and N is that the coherent state (amplitude)^2 has a natural period $2M$ in variable p instead of the usual period M when $MN=$even.

2. $MN=$even, arbitrary n

For the present case

$$2\pi\hbar = nM/(nM), \quad MN = \text{even} , \tag{A19}$$

we consider an $nN\times nN$ finite unitary matrix

$$U(a)_{ss'} = \sum_l U_{s,s'+nlN} e^{-inla} , \tag{A20}$$

with

$$1\le s,s'\le nN . \tag{A21}$$

The $U_{ss'}$ obeys

$$U(a)_{s+N,s'+N} = U(a)_{ss'} . \tag{A22}$$

When either $s+N$ or $s'+N$ becomes larger than nN, we have

$$U(a)_{s+nN,s'} = e^{-ina}U(a)_{ss'} , \tag{A23a}$$

$$U(a)_{s,s'+nN} = e^{ina}U(a)_{ss'} . \tag{A23b}$$

Using (A22) and (A23), we can express this $nN\times nN$ matrix U into a block matrix made of $n\times n$ submatrices,

$$U = \begin{bmatrix} u_1 & e^{ia}u_2 & e^{2ia}u_3 & \cdots & e^{i(n-1)a}u_n \\ e^{-ia}u_n & u_1 & e^{ia}u_2 & \cdots & e^{i(n-2)a}u_{n-1} \\ \cdots & \cdots & \cdots & \cdots & \cdots \\ e^{-i(n-1)a}u_2 & e^{-i(n-2)a}u_3 & \cdots & \cdots & u_1 \end{bmatrix} \tag{A24}$$

where each submatrix u_i is an $N\times N$ matrix. The condition that U is unitary implies

$$\sum_{r=1}^{n} u_{r+k}^{\dagger} u_r = \delta_{k0} I \ , \tag{A25}$$

where I is the $N\times N$ identity matrix, and the index r in u_r is treated cyclically,

$$u_{n+r}=u_r, u_{n+r}^{\dagger}=u_r^{\dagger} \ . \tag{A26}$$

It is easy to see that U is a unitary transformation of a simpler matrix V,

$$U=P^{\dagger}VP \ , \tag{A27}$$

with

$$V=\begin{pmatrix} u_1 & u_2 & \cdots & u_n \\ u_n & u_1 & \cdots & u_{n-1} \\ \cdots & \cdots & \cdots & \cdots \\ u_2 & u_3 & \cdots & u_1 \end{pmatrix} \tag{A28}$$

and

$$P=\begin{pmatrix} e^{ia} & 0 & \cdots & 0 \\ 0 & e^{2ia} & \cdots & 0 \\ \cdots & \cdots & \cdots & \cdots \\ 0 & 0 & \cdots & e^{ina} \end{pmatrix} . \tag{A29}$$

From (A27), we can obtain an eigenstate of U from an eigenstate of V. The two matrices have the same eigenvalues.

We can reduce the eigenvalue problem of V to that of diagonalizing $N\times N$ matrices as follows. We define an $N\times N$ matrix

$$u(\theta)\equiv \sum_{r=1}^{n} u_r e^{-ir\theta} \ , \tag{A30}$$

with θ obeying

$$e^{in\theta}=1 \ . \tag{A31}$$

Let $\phi(\theta)$ be the eigenstate of $u(\theta)$,

$$u(\theta)\phi(\theta)=e^{-i\omega(\theta)}\phi(\theta) \ . \tag{A32}$$

Then, the eigenstate of V and U for the same eigenvalue $e^{-i\omega(\theta)}$ are

$$\psi_V=\begin{pmatrix} e^{-\theta} \\ e^{-2i\theta} \\ \vdots \\ e^{-in\theta} \end{pmatrix}\phi(\theta) \ , \tag{A33}$$

$$\psi_U=\begin{pmatrix} e^{-i(\theta+a)} \\ e^{-2i(\theta+a)} \\ \vdots \\ e^{-in(\theta+a)} \end{pmatrix}\phi(\theta) \ , \tag{A34}$$

respectively.

We can generalize our reduction method straightforwardly to cover the remaining case of $MN=$odd and $n>2$.

[1]For a review of the classical Chirikov map, see B. V. Chirikov, Phys. Rep. **52**, 263 (1979); J. Greene, J. Math. Phys. **20**, 1183 (1979).

[2]A. N. Kolmogorov, Dokl. Akad. Nauk SSSR **98**, 527 (1954); V. I. Arnol'd, Russ. Math. Surv. **18**, 85 (1963); J. Moser, Nachr. Akad. Wiss. Goettingen Math. Phys. Kl. **2**, 1 (1962).

[3]For the application of nonlinear dynamics to accelerator physics, see *Nonlinear Dynamics and the Beam-Beam Interaction (Brookhaven National Laboratory, 1979)*, Proceedings of the Symposium on Nonlinear Dynamics and the Beam-Beam Interaction, AIP Conf. Proc. No. 57, edited by M. Month and J. C. Herrera (AIP, New York, 1979); *Physics of High-Energy Particle Accelerators (Fermilab Summer School, 1981)*, Proceedings of the Summer School on High-Energy Particle Accelerators, AIP Conf. Proc. No. 87, edited by R. A. Carrigan, F. R. Huson, and M. Month (AIP, New York, 1982).

[4]G. Casati, B. V. Chirikov, F. M. Izraelev, and J. Ford, in *Stochastic Behavior in Classical and Quantum Hamiltonian Systems*, Vol. 93 of *Lecture Notes in Physics*, edited by C. Casati and J. Ford (Springer, New York, 1979).

[5]F. M. Izrailev and D. L. Shepelyanskii, Dokl. Akad. Nauk SSSR **249**, 1103 (1979) [Sov. Phys.—Dokl. **24**, 996 (1979)]. See also B. Dorizzi *et al.*, J. Stat. Phys. **37**, 93 (1984).

[6]For an up-to-date review of quantum iterative systems, see J. Bellisard's paper in *Trends and Developments in the Eighties*, edited by S. Albeverio and Ph. Blanchard (World Scientific, Singapore, 1985).

[7]D. R. Grempel, S. Fishman, and R. E. Prange, Phys. Rev. Lett. **49**, 833 (1982); D. R. Grempel, R. E. Prange, and S. Fishman, Phys. Rev. A **29**, 1639 (1984).

[8]M. V. Berry, Physica **10D**, 369 (1984).

[9]G. Casati and I. Guarneri, Commun. Math. Phys. **95**, 121 (1984).

[10]For discussions on quantum recurrence, see, e.g., T. Hogg and B. A. Huberman, Phys. Rev. Lett. **48**, 711 (1982); Phys. Rev. A **28**, 22 (1983). See also H. A. Cerderia, Phys. Rev. A **30**, 1752 (1984); D. R. Grempel *et al.*, in Ref. 7, and B. Dorizzi *et al.*, in Ref. 5.

[11]E. Wigner, Phys. Rev. **40**, 749 (1932).

[12]M. V. Berry *et al.*, Ann. Phys. (N.Y.) **122**, 26 (1979); M. V. Berry, J. Phys. A **10**, 2083 (1977).

[13]S. J. Chang and K. J. Shi (unpublished).

[14]S. J. Chang and K. J. Shi, Phys. Rev. Lett. **55**, 269 (1985).

[15]It is easy to show that the quantization rules given in this section are equivalent to introducing the Schrödinger equation via (2.1). See F. M. Izrailev and D. L. Shepelyanskii in Ref. 5.

[16]For general descriptions of a dynamical system periodic in both p and q, see J. Schwinger, *Quantum Kinematics and Dynamics* (Benjamin, New York, 1970); J. Schwinger, Proc. Natl. Acad. Sci. **46**, 570 (1960); J. H. Hannay and M. V. Berry, Physica **1D**, 267 (1980).

[17]The energy of the rotor is $E_n = \hbar\omega n^2/2$.

[18]For the integral form of the Poisson sum formula, see, e.g., G. F. Carrier *et al.*, *Functions of a Compex Variable* (McGraw-Hill, New York, 1966), pp. 310—312.

[19]R. J. Glauber, Phys. Rev. **131**, 2766 (1963).

[20]N. D. Cartwright, Physica **83A**, 210 (1976); A. K. Rajagopal, Phys. Rev. A **27**, 558 (1983).

[21]Absence of level crossings and the presence of level distributions following those of Gaussian orthogonal random matrices are important indications of quantum chaos. See, e.g., S. W. McDonald and A. N. Kaufman, Phys. Rev. Lett. **42**, 1189 (1979); M. V. Berry *et al.*, Ann. Phys. (N.Y.) **131**, 163 (1981); O. Bohigas *et al.*, Phys. Rev. Lett. **52**, 1 (1984); T. H. Seligman *et al.*, *ibid.* **53**, 215 (1984).

[22]See, e.g., B. Simon, Adv. Appl. Math. **3**, 463 (1982); Y. G. Sinai, Func. Anal. Appl. **19**, 42 (1985) (English translation, pp. 34—39).

[23]K. Takahashi and T. Saito [Phys. Rev. Lett. **55**, 645 (1985)] also reach the same conclusion.

[24]For a partial list of possible descriptions of quantum chaos, see, e.g., M. Shapiro and G. Goelman, Phys. Rev. Lett. **53**, 1714 (1984); A. Peres, *ibid.* **53**, 1711 (1984).

[25]F. M. Izrailev, Phys. Rev. Lett. **56**, 541 (1986).

[26]R. Kosloff and S. A. Rice, J. Chem. Phys. **74**, 1340 (1981); R. M. Stratt *et al.*, *ibid.* **71**, 3311 (1979).